Journal of Alloys and Compounds 509 (2011) 8716–8719

Contents lists available at ScienceDirect

Journal of Alloys and Compounds

journal homepage: www.elsevier.com/locate/jallcom

High permittivity and low dielectric loss of the $Ca_{1-x}Sr_xCu_3Ti_4O_{12}$ ceramics

Zupei Yang*, Lijuan Zhang, Xiaolian Chao, Lirong Xiong, Jie Liu

Key Laboratory for Macromolecular Science of Shaanxi Province, School of Chemistry and Materials Science, Shaanxi Normal University, Xi'an 710062, Shaanxi, PR China

ARTICLE INFO

Article history:
Received 21 December 2010
Received in revised form 13 June 2011
Accepted 13 June 2011
Available online 17 June 2011

Keywords:
Ceramics
X-ray diffraction
Microstructure
Dielectric properties

ABSTRACT

The $Ca_{1-x}Sr_xCu_3Ti_4O_{12}$ (CSCTO) giant dielectric ceramics were prepared by conventional solid-state method. X-ray diffraction patterns revealed that a small amount of Sr^{2+} ($x < 0.2$) had no obvious effect on the phase structure of the CSCTO ceramics, while with increasing the Sr^{2+} content, a second phase of $SrTiO_3$ appeared. Electrical properties of CSCTO ceramics greatly depended on the Sr^{2+} content. The $Ca_{0.9}Sr_{0.1}Cu_3Ti_4O_{12}$ ceramics exhibited a higher permittivity (71,153) and lower dielectric loss (0.022) when measured at 1 kHz at room temperature. The ceramics also performed good temperature stability in the temperature range from −50 °C to 100 °C at 1 kHz. By impedance spectroscopy analysis, all compounds were found to be electrically heterogeneous, showing semiconducting grains and insulating grain boundaries. The grain resistance was 1.28 Ω and the grain boundary resistance was 1.31×10^5 Ω. All the results indicated that the $Ca_{0.9}Sr_{0.1}Cu_3Ti_4O_{12}$ ceramics were very promising materials with higher permittivity for practical applications.

1. Introduction

Perovskite $CaCu_3Ti_4O_{12}$ (CCTO) has attracted much attention because of its intriguing mechanism and potential technical applications in microelectronic devices. Since $CaCu_3Ti_4O_{12}$ (CCTO) giant dielectric material was reported by Subramanian et al. in 2000, CCTO has attracted considerable attention owing to its high dielectric permittivity ($\sim 10^4$–10^5) at low frequencies and room temperature [1–6]. CCTO simultaneously has good temperature stability over a wide temperature ranging from 100 K to 600 K [7]. At temperature below 100 K, the dielectric constant drops rapidly to around 100 without any structural phase transition [8,9]. Despite the fact that much research work has been done, including the experiment and theory, to reveal the origin of the giant dielectric permittivity of CCTO ceramics, it still remains controversial and unsolved problems to date. For CCTO ceramics, the internal barrier layer capacitance (IBLC) model is commonly accepted as the nature of its giant dielectric response. Sinclair et al. reported that CCTO ceramics consisting of semiconducting grains and insulating grain boundaries were electrically heterogeneous [8].

Up to now, several investigation on the CCTO ceramics and single crystal as well as other related materials have been reported, but the high loss tangent ($\tan\delta$) of the CCTO ceramics ($\tan\delta > 0.05$ at 1 kHz) is still an obstruction to the technical use of the CCTO. Number of attempts has been made to decease $\tan\delta$ by various compositional modifications, such as TeO_2-doped CCTO [10], ZrO_2-doped CCTO [11], CCTO/$CaTiO_3$ composite [12,13], TiO_2-rich CCTO [14], and the substitution of La for Cu in CCTO [15] have also been reported to be effective in reducing the dielectric loss and still maintaining the high dielectric constant.

In this work, the cations substitution in the A site of CCTO by Sr^{2+} has been studied. The phase structure, microstructure, electrical properties of the CSCTO ceramics were investigated.

2. Experimental

$Ca_{1-x}Sr_xCu_3Ti_4O_{12}$ ($x = 0$, 0.10, 0.15, 0.20, 0.25) ceramics were prepared by the conventional solid-state method. $CaCO_3$ (99.99%), $SrCO_3$ (99.99%), CuO (99.99%), and TiO_2 (99.99%) were used as starting materials. The stoichiometric powders were mixed by ball-milled in ethanol for 10 h using agate balls. The mixed powders were calcined at 900 °C for 10 h in air and then pressed into disks with a diameter of 15 mm under 100 MPa pressure using a solution of poly vinyl alcohol (PVA) as binder. The pellets were sintered at 1060 °C, 1080 °C, 1090 °C and 1100 °C for 5 h in air, respectively.

The crystalline phase of the sintered specimens was identified by X-ray diffraction (XRD, D/max-2550/PC, Rigaku, Japan) technique using Cu Kα radiation, and the surface microstructure was observed by scanning electron microscopy (SEM, Quanta 200, Philips, Netherlands). In order to measure the electric properties, silver paste was painted on both sides of samples as the electrodes and were fired at 840 °C, and then the samples were measured by Agilent 4294A impedance analyzer in the frequency ranging from 40 Hz to 110 MHz.

3. Results and discussion

Fig. 1 shows the XRD patterns of CSCTO powders with different Sr^{2+} contents calcined at 900 °C for 10 h. It can be seen from Fig. 1 that the samples of $x < 0.2$ are single CCTO phase, which could be

* Corresponding author. Tel.: +86 29 8531 0352; fax: +86 29 8530 7774.
E-mail address: yangzp@snnu.edu.cn (Z. Yang).

0925-8388/$ – see front matter © 2011 Elsevier B.V. All rights reserved.
doi:10.1016/j.jallcom.2011.06.039

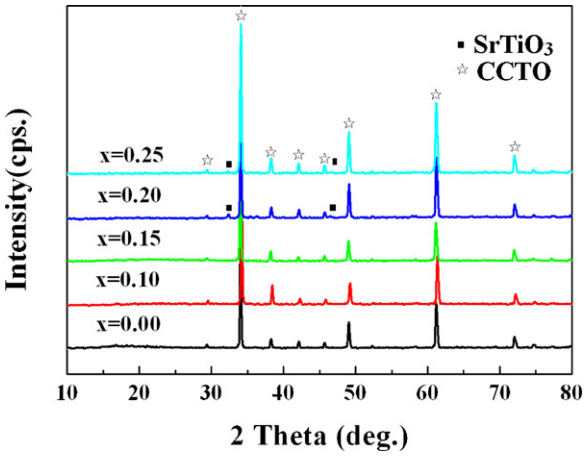

Fig. 1. X-ray diffraction patterns of $Ca_{1-x}Sr_xCu_3Ti_4O_{12}$ as a function of Sr^{2+} doping.

indexed to a cubic perovskite-related structure according to JCPDS-75-2188 [16], indicating that a little amount of Sr^{2+} can enter into the lattice of CCTO. For the samples of $x \geq 0.2$, some diffraction peaks of the second phase were found around $2\theta \sim 32.5^\circ$, 46.7°, which means a small amount of $SrTiO_3$ impurity phase starts to appear. The ionic radius of Sr^{2+} ($r_{Sr^{2+}} = 1.44$ Å) is close to that of Ca^{2+} ($r_{Ca^{2+}} = 1.34$ Å), then small amount of Sr^{2+} can easily enter into the structure lattice and form a solid solution, while with increasing the Sr^{2+} content, the second phase of $SrTiO_3$ appears.

Fig. 2 demonstrates the SEM images of CSCTO ceramics sintered at 1080 °C with various x values. Abnormal grain growth with grain size larger than 100 μm can be found in Fig. 2(a)–(c). With increasing Sr^{2+} content, the average grain size of CSCTO ceramics increases firstly and then decreases. The average grain size of $Ca_{0.9}Sr_{0.1}Cu_3Ti_4O_{12}$ ceramics is about 150–200 μm, which is greater than that of other doped samples. In addition, normal grain growth, clear grain boundaries and the porosities can be obtained only in Fig. 2(d), which shows that further increasing x to 0.25 can lead to the decrease of grain size and disappearance of abnormal grain growth.

Fig. 3(a) illustrates the frequency dependence of the permittivity (ε_r) of the CSCTO ceramics with different x values measured at room temperature. It exhibits the plateaus permittivity of the CSCTO ceramics at the frequency ranging from 40 Hz to 100 kHz. When the frequency surpasses 100 kHz, the permittivity drastically decreases and then almost turns to be a small constant. The results show that the CSCTO ceramics have good frequency stability. This is a typical characteristic of Debye relaxation, and it is consistent with the reported results [17–20]. In addition, the permittivity of ceramics with $x = 0.15$–0.25 (below 13,000) is smaller than the values of sample with $x = 0$, 0.1 (above 70,000). It can also be seen that the $Ca_{0.9}Sr_{0.1}Cu_3Ti_4O_{12}$ ceramics have higher permittivity (71,153) at 1 kHz than that of the CCTO (61,425) ceramics. The giant permittivity can be explained as an internal barrier layer capacitance (IBLC)

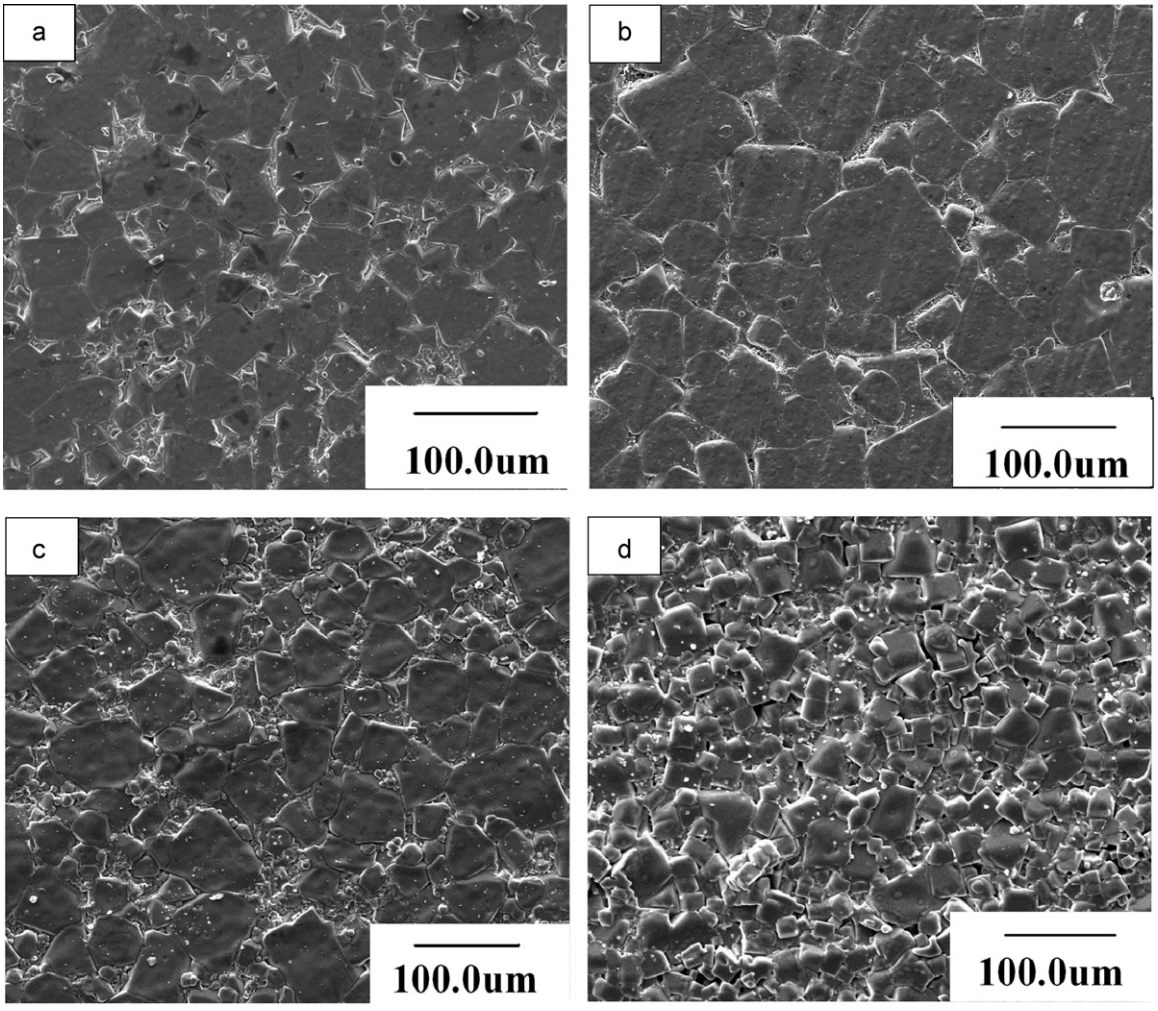

Fig. 2. Surface SEM images of $Ca_{1-x}Sr_xCu_3Ti_4O_{12}$ ceramics: (a) $x = 0.00$, (b) $x = 0.10$, (c) $x = 0.15$, (d) $x = 0.25$.

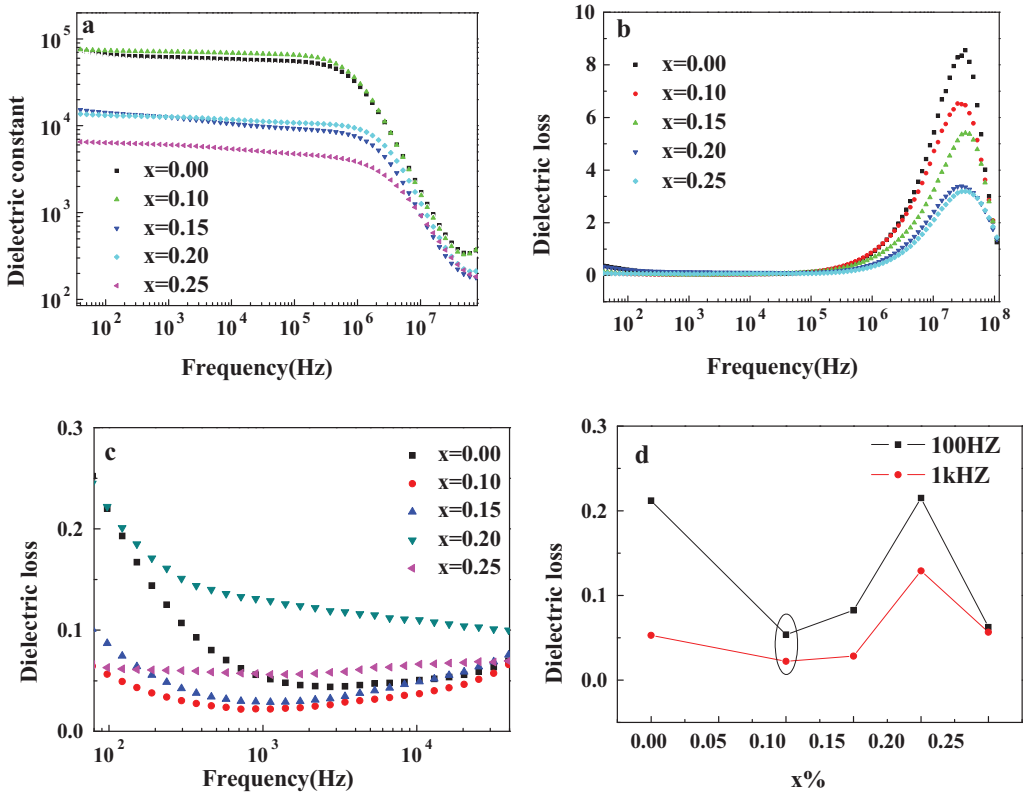

Fig. 3. Frequency dependence of permittivity (a) and dielectric loss (b) of $Ca_{1-x}Sr_xCu_3Ti_4O_{12}$ ceramics at room temperature, Fig. 3(c) is a magnified view of dielectric loss from 100 Hz to 40 kHz, the dielectric loss at 100 Hz and 1000 Hz with different Sr^{2+} content is shown in Fig. 3(d).

effect by Ferrarelli et al. [21]. Consequently, appropriately substituting Ca^{2+} with Sr^{2+} in CCTO can improve the dielectric properties of the ceramics.

The frequency dependence of dielectric loss of the CSCTO ceramics as a function of x measured at room temperature is shown in Fig. 3(b). It is evident that the dielectric loss has good frequency stability from 40 Hz to 100 kHz. As the frequency increases above 100 kHz, dielectric loss drastically increases and then decreases. It can also be found that the dielectric loss of the CSCTO ceramics gradually reduces with increasing the Sr^{2+} content in the frequency from 1.6 MHz to 56 MHz. Fig. 3(c) is a magnified view of dielectric loss from 100 Hz to 40 kHz, dielectric loss decreases and then increases with the Sr^{2+} content in Fig. 3(c). The dielectric loss at 100 Hz and 1 kHz with different Sr^{2+} content is shown in Fig. 3(d). It can be seen from Fig. 3(d) that the $Ca_{0.9}Sr_{0.1}Cu_3Ti_4O_{12}$ ceramics possess the lowest dielectric loss (0.0537) at 100 Hz and (0.022) at 1 kHz. With reference to Fig. 3(a) and (b), the $Ca_{0.9}Sr_{0.1}Cu_3Ti_4O_{12}$ ceramics have higher permittivity (about 71,153) and lower dielectric loss (about 0.022) at 1 kHz at room temperature.

It is well known that the impedance spectroscopy (IS) is a powerful tool in separating out the grain and the grain boundary effects. For CCTO ceramics, an impedance spectroscopy analysis demonstrates that CCTO ceramics are electrically heterogeneous, consisting of semiconducting grains and insulating grain boundaries, which are simulated by Zsimp Win software. The impedance of electroceramics has been modeled as an equivalent circuit consisting of two parallel *RC* elements connected in series, of which one RC element corresponds to the semiconducting grains and the other corresponds to the insulating grain boundaries. For such a circuit, each RC element ideally gives rise to semicircular arc in complex impedance plane Z^* [22], where

$$Z^* = Z' - iZ''$$

where

$$Z' = \frac{R_g}{1+(\omega R_g C_g)^2} + \frac{R_{gb}}{1+(\omega R_{gb} C_{gb})^2}$$

and

$$Z'' = R_g\left[\frac{\omega R_g C_g}{1+(\omega R_g C_g)^2}\right] + R_{gb}\left[\frac{\omega R_{gb} C_{bg}}{1+(\omega R_{gb} C_{gb})^2}\right]$$

R_g and C_g represent the grain resistance and capacitance, respectively, while R_{gb} and C_{gb} represent the grain boundary resistance and capacitance, respectively.

Fig. 4 shows complex impedance spectroscopy of CSCTO ceramics with various x values. The R_g and R_{gb} values can be obtained by an impedance spectrum analysis. The data of all CSCTO ceramics shows a single semicircular arc with a nonzero high frequency intercept. There are two semicircular arcs in the complex impedance spectroscopy in the measuring frequency ranging from 40 Hz to 110 MHz, corresponding to the two parallel RC elements in series, which indicates that the higher permittivity is due to IBLC model [23,24]. The IS results show the high frequency impedance corresponds to grain resistance R_g and the low frequency impedance corresponds to grain boundary resistance R_{gb}. As the frequency increases, grain boundary resistance (R_{gb}) and grain resistance (R_g) first increase and then decrease. As is shown in Fig. 4, the grain resistance (R_g) of the $Ca_{0.9}Sr_{0.1}Cu_3Ti_4O_{12}$ ceramics is 1.28 Ω and the grain boundary resistance (R_{gb}) is 1.31×10^5 Ω. Generally, the grain resistance R_g is much smaller than the grain boundary resistance R_{gb}. These results indicate that the grains are semiconducting and the grain boundaries are insulating, which is consistent with the internal barrier layer capacitance (IBLC) model and demonstrates that CSCTO ceramics are electrically heterogeneous. The R_{gb} has the similar change trend as R_g and the maximum

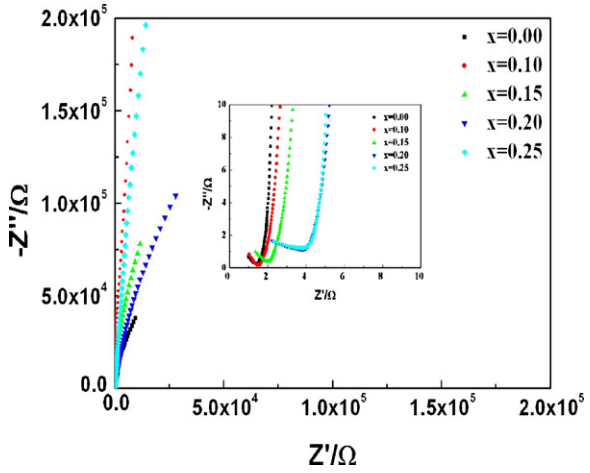

Fig. 4. The Cole–Cole plot of impedance at room temperature for $Ca_{1-x}Sr_xCu_3Ti_4O_{12}$ ceramics. The inset shows an enlarged view for the highest frequency data close to the origin.

value of R_{gb} and R_g of the $Ca_{0.9}Sr_{0.1}Cu_3Ti_4O_{12}$ ceramics can be seen in Fig. 4. Experimental results are basically consistent with the reduction in dielectric loss, the dielectric loss is approximately written by Eq. (1) [25]

$$\tan\delta = \frac{1}{wR_{gb}C} + wR_gC \quad (1)$$

where C and w represent measured capacitance and angle frequency, respectively. It can be seen that the first term on the right of Eq. (1) has higher weight at low frequencies, while the second term becomes predominant at high frequencies, due to $R_{gb} \geq R_g$. According to Eq. (1), $\tan\delta \approx 1/wR_{gb}C$ at low frequencies, while $w > 10^5$ Hz, $\tan\delta \approx wR_gC$. This is in conformity with the decrease of dielectric loss in Fig. 3(b) and (c). Based on IBLC model, this phenomenon suggests that the Sr^{2+} affects the electrical properties of CCTO.

Fig. 5 shows the temperature dependence of the permittivity and dielectric loss of the CCTO and the $Ca_{0.9}Sr_{0.1}Cu_3Ti_4O_{12}$ ceramics at 1 kHz from −50 °C to 100 °C. The results reveal that the CCTO and $Ca_{0.9}Sr_{0.1}Cu_3Ti_4O_{12}$ ceramics have higher permittivity (above 60,000) and lower dielectric loss (below 0.05) with good temperature stability in the temperature ranging from −50 °C to 50 °C. Further increasing the temperature leads to the increase in both permittivity and dielectric loss. Compared with CCTO ceramics, the $Ca_{0.9}Sr_{0.1}Cu_3Ti_4O_{12}$ ceramics have better temperature stability.

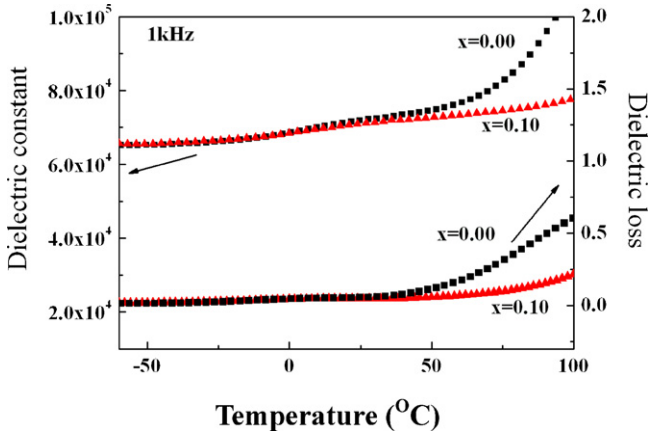

Fig. 5. Temperature dependence of dielectric properties of $Ca_{1-x}Sr_xCu_3Ti_4O_{12}$ (x = 0.00, 0.10) specimens at 1 kHz.

4. Conclusions

$Ca_{1-x}Sr_xCu_3Ti_4O_{12}$ ($0 \leq x \leq 0.25$) giant dielectric ceramics were prepared by the conventional solid-state method. The phase structure, microstructure and dielectric properties of CSCTO ceramics were investigated. XRD results indicated that when $x < 0.2$, Sr^{2+} could enter into the cubic perovskite structure lattice and form a solid solution, while with increasing the Sr^{2+} content, the second phase of $SrTiO_3$ appeared. Scanning electron microscopy analysis showed that the grains of CSCTO (x = 0.10) ceramics were greater than that of CCTO and the grains of CSCTO (x > 0.10) ceramics gradually decreased with increasing the Sr^{2+} content. The permittivity and the dielectric loss of the $Ca_{0.9}Sr_{0.1}Cu_3Ti_4O_{12}$ ceramics were 71,153 and 0.022, respectively when measured at 1 kHz at room temperature. The permittivity of the $Ca_{0.9}Sr_{0.1}Cu_3Ti_4O_{12}$ ceramics was more than 65,000 and corresponding dielectric loss was below 0.05 at 1 kHz in the range of −50 °C to 100 °C. The results indicated that the $Ca_{0.9}Sr_{0.1}Cu_3Ti_4O_{12}$ ceramics performed higher permittivity, lower dielectric loss and better temperature stability. The experimental results were consistent with the simulated data obtained from Zsimp Win software, which demonstrated that the $Ca_{0.9}Sr_{0.1}Cu_3Ti_4O_{12}$ ceramics were electrically heterogeneous. All results indicated that the $Ca_{0.9}Sr_{0.1}Cu_3Ti_4O_{12}$ ceramics were very promising materials with higher permittivity and lower dielectric loss for practical applications.

Acknowledgements

This work was supported by National Science Foundation of China (NSFC) (Grant No. 20771070), Natural Science Research Program of Shaanxi Province (Grant No. 2009JZ003), Fundamental Research Funds for the Central Universities (Program No. GK200901003).

References

[1] M.A. Subramanian, D. Li, N. Duan, B.A. Reisner, A.W. Sleight, J. Solid State Chem. 151 (2000) 323–325.
[2] C.C. Homes, T. Vogt, S.M. Shapiro, S. Wakimoto, A.P. Ramirez, Science 293 (2001) 673.
[3] A.P. Ramirez, M.A. Subramanian, M. Gardel, G. Blumberg, D. Li, T. Vogt, S.M. Shapiro, Solid State Commun. 115 (2000) 217.
[4] M.A. Subramanian, A.W. Sleight, Solid State Sci. 4 (2002) 347–351.
[5] C.C. Homes, T. Vogt, S.M. Shapiro, Phys. Rev. B 67 (2003) 092106.
[6] A.R. West, T.B. Adams, F.D. Morrison, D.C. Sinclair, J. Eur. Ceram. Soc. 24 (2004) 1439–1448.
[7] C.H. Mu, P. Liu, Y. He, J.P. Zhou, H.W. Zhang, J. Alloys Compd. 471 (2009) 137–141.
[8] D.C. Sinclair, T.B. Adams, F.D. Morrison, A.R. West, Appl. Phys. Lett. 80 (2002) 12.
[9] V. Brizé, G. Gruener, J. Wolfman, K. Fatyeyeva, M. Tabellout, M. Gervais, F. Gervais, Mater. Sci. Eng. B 129 (2006) 135–138.
[10] F. Amaral, L.C. Costa, M.A. Valente, J. Non-cryst. Solids 357 (2011) 775–781.
[11] E.A. Patterson, S. Kwon, C.C. Huang, Appl. Phys. Lett. 87 (2005) 182911–182913.
[12] C.-M. Wang, S.-Y. Lin, K.-S. Kao, Y.-C. Chen, S.-C. Weng, J. Alloys Compd. 491 (2010) 423–430.
[13] L. Ramajo, R. Parraa, J.A. Varela, M.M. Reboredo, M.A. Ramire, M.S. Castro, J. Alloys Compd. 497 (2010) 349–353.
[14] Ashutosh Kumar Dubey, Prakash Singh, Sindhu Singh, Devendra Kumar, Om Parkash, J. Alloys Compd. 509 (2011) 3899–3906.
[15] W. Makcharoen, J. Tontrakoon, G. Rujijanagul, D.P. Cann, T. Tunkasiri, Ceram. Int. 10 (2010) 1016.
[16] W.Q. Ni, X.H. Zheng, J.C. Yu, J. Mater. Sci. 42 (2007) 1037–1041.
[17] L. Feng, M. Shen, W.W. Cao, J. Appl. Phys. 95 (2004) 6483.
[18] R.N. Choudhary, U. Bhunia, J. Mater. Sci. 37 (2002) 5177.
[19] S.M. Moussa, B.J. Kennedy, Mater. Res. Bull. 36 (2001) 2525.
[20] H. Birey, J. Appl. Phys. 49 (1978) 2898.
[21] M.C. Ferrarelli, D.C. Sinclair, A.R. West, Appl. Phys. Lett. 94 (2009) 212901.
[22] D.C. Sinclair, A.R. West, J. Appl. Phys. 66 (1989) 3850.
[23] J. Li, A.W. Sleight, M.A. Subramanian, Solid State Commun. 135 (2005) 260–262.
[24] T.B. Adams, D.C. Sinclair, A.R. West, Adv. Mater. 14 (2002) 1321.
[25] Y.Y. Yan, L.X. Feng, G.H. Cao, Mater. Sci. Eng., B: Solid-State Mater. Adv. Technol. 130 (2006).